

# Quantum effects in a weakly-frustrated $S=1/2$ two-dimensional Heisenberg antiferromagnet in an applied magnetic field

N. Tsyrlin<sup>1,2</sup>, T. Pardini<sup>3</sup>, R. R. P. Singh<sup>3</sup>, F. Xiao<sup>4</sup>, P. Link<sup>5</sup>, A. Schneidewind<sup>5,6</sup>, A. Hiess<sup>7</sup>, C. P. Landee<sup>4</sup>, M. M. Turnbull<sup>8</sup>, M. Kenzelmann<sup>1,9</sup>

(1) Laboratory for Solid State Physics, ETH Zurich, CH-8093 Zurich, Switzerland

(2) Laboratory for Neutron Scattering, ETH Zurich & Paul Scherrer Institute, CH-5232 Villigen, Switzerland

(3) Department of Physics, University of California, Davis, Davis, California 95616, USA

(4) Department of Physics, Clark University, Worcester, Massachusetts 01610, USA

(5) Forschungsneutronenquelle Heinz Maier-Leibnitz (FRM II), D-85747 Garching, Germany

(6) Institut für Festkörperphysik, TU Dresden, D-01062 Dresden, Germany

(7) Institut Laue-Langevin, Boîte Postale 156, F-38042 Grenoble, France

(8) Carlson School of Chemistry and Biochemistry,

Clark University, Worcester, Massachusetts 01610, USA

(9) Laboratory for Developments and Methods, Paul Scherrer Institute, CH-5232 Villigen, Switzerland

We have studied the two-dimensional  $S=1/2$  square-lattice antiferromagnet  $\text{Cu}(\text{pz})_2(\text{ClO}_4)_2$  using neutron inelastic scattering and series expansion calculations. We show that the presence of antiferromagnetic next-nearest neighbor interactions enhances quantum fluctuations associated with resonating valence bonds. Intermediate magnetic fields lead to a selective tuning of resonating valence bonds and a spectacular inversion of the zone-boundary dispersion, providing novel insight into 2D antiferromagnetism in the quantum limit.

PACS numbers:

Some of the best examples of macroscopic quantum magnets can be found in low-dimensional antiferromagnets that preserve strong quantum fluctuations to very low temperatures. Cases in point are antiferromagnetic (AF) chains that are quantum critical at zero temperature and feature deconfined spinon excitations for  $S=1/2$  [1], but a spin liquid with gapped triplet excitations for  $S=1$  [2]. In two dimensions, quantum effects are generally reduced and the ground state of  $S=1/2$  square lattice Heisenberg antiferromagnets is long-range ordered, albeit with a reduced ordered moment and spin-waves whose energy is renormalized by quantum fluctuations [3, 4]. Importantly, however, short range quantum correlations are preserved in the ground state and lead to a quantum-induced dispersion at the AF zone boundary and to a weak continuum of states at high energies [4, 5, 6, 7, 8, 9, 10, 11, 12].

Competing interactions generally increase quantum fluctuations, particularly for materials close to a quantum critical point. For the 2D  $S=1/2$  antiferromagnet, one source of competition can be next-nearest neighbor interactions that destabilize a simple nearest-neighbor antiparallel alignment and thus enhance fluctuations [13, 19]. Such a scenario has been extensively investigated using the  $J_1 - J_2$  model, where  $J_1$  and  $J_2$  give the strength of the nearest and next-nearest neighbor interactions [13]. The  $J_1 - J_2$  model features two different types of order for  $J_2/J_1 < 0.38$  and  $J_2/J_1 > 0.6$ , and probably a spin-liquid phase in between. The behavior of the 2D  $S=1/2$  antiferromagnet in magnetic fields was studied theoretically for the case of nearest neighbor interactions [14, 15, 16] as well as for  $J_1 - J_2$  model [17, 18]. However, little is known experimentally about the magnetic field

behavior of the 2D  $S=1/2$  antiferromagnet, particularly in the presence of next-nearest neighbor interactions.

We have studied a weakly-frustrated  $S=1/2$  AF square-lattice where next-nearest neighbor interactions are a small perturbation that allows us to study the change of the magnetic properties upon introduction of competing interactions. Our inelastic neutron scattering experiments were performed using the 2D square lattice Heisenberg antiferromagnet  $\text{Cu}(\text{pz})_2(\text{ClO}_4)_2$ . Deuterated  $\text{Cu}(\text{pz})_2(\text{ClO}_4)_2$  crystallizes in the monoclinic  $C2/c$  space group [20]. Each  $\text{Cu}^{2+}$  ion in  $\text{Cu}(\text{pz})_2(\text{ClO}_4)_2$  carries  $S=1/2$  and is surrounded by two pairs of identical cis pyrazine molecules, creating a two dimensional square array of copper atoms linked by pyrazine molecules in the  $bc$  plane. The two fold rotation axis  $(0, y, 1/2)$  and the mirror plane parallel to the  $ac$  plane ensures that all nearest neighbor interactions between  $\text{Cu}^{2+}$  ions on the square lattice are identical. From the temperature dependence of the magnetic susceptibility, it was concluded that  $\text{Cu}(\text{pz})_2(\text{ClO}_4)_2$  represents a  $S=1/2$  2D square lattice antiferromagnet with nearest-neighbor exchange  $J = 1.53(8)$  meV and a saturation field of  $\mu_0 H_{\text{sat}} \sim 45$  T [21, 22]. Due to interplane interactions,  $\text{Cu}(\text{pz})_2(\text{ClO}_4)_2$  adopts long-range AF order below  $T_N = 4.2$  K and the ratio between the interlayer to intralayer exchange has been estimated as  $J'/J = 6.8 \cdot 10^{-4}$  [20, 22].

The neutron experiments were performed using the cold-neutron triple-axis spectrometers PANDA at FRM2 at Garching and IN14 at ILL at Grenoble, and an array of deuterated  $\text{Cu}(\text{pz})_2(\text{ClO}_4)_2$  single crystals with a total mass up to 2g co-aligned with a mosaic of  $0.5^\circ$ . The sample was aligned with its reciprocal  $(0, k, l)$  plane in the horizontal scattering plane. A cryomag-

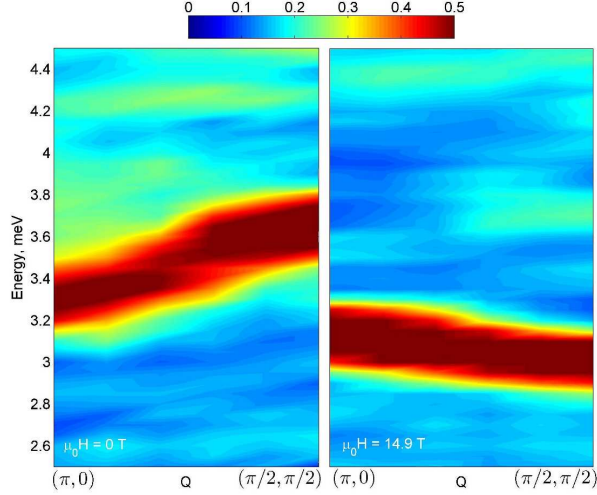


FIG. 1: Zone boundary spin dispersion at zero field and  $\mathbf{H} \sim \mathbf{J}$ . Color plot of the normalized scattering intensity  $I(\mathbf{Q}, \omega)$  at  $T = 80$  mK, showing the dispersion from  $(\pi, 0)$  to  $(\pi/2, \pi/2)$  at zero field and  $\mu_0 H = 14.9$  T under otherwise identical conditions. Both panels present smoothed data obtained by performing six constant  $\mathbf{Q}$ -scans from  $(\pi/2, \pi/2)$  to  $(\pi, \pi)$  with a 0.05 meV energy step.

net allowed the application of vertical magnetic fields up to 14.9 T. The magnetic field was thus nearly perpendicular to the square-lattice plane. To probe the ground state as a function of magnetic field, we used a dilution refrigerator, reaching temperatures of the order of 50-100 mK in each of the two experiments. The measurements were performed using a fixed final energy  $E_f = 4.66$  meV and  $E_f = 2.98$  meV for the PANDA and IN14 experiments, respectively, obtained via the (002) Bragg reflection from a pyrolytic graphite (PG) monochromator, a focused analyzer and a cooled Be filter before the analyzer. The chemical unit cell contains four  $\text{Cu}^{2+}$  atoms, thus nearest-neighbor AF order does not break translational invariance, and  $\mathbf{Q} = (0, 1, 0)$  and  $\mathbf{Q} = (0, 0, 1)$  correspond to the AF point  $(\pi, \pi)$ . Consequently,  $\mathbf{Q} = (0, m \pm 1/2, n \pm 1/2)$ , where  $m$  and  $n$  are integers, correspond to  $(\pi, 0)$ , while  $\mathbf{Q} = (0, m \pm 1/2, n)$  corresponds to  $(\pi/2, \pi/2)$ .

A color plot of the normalized neutron scattering spectra at the zone boundary is shown in Fig. 1 for zero applied field and  $\mu_0 H = 14.9$  T. At zero field, the onset of scattering at reciprocal wave-vector  $(\pi, 0)$  is reduced by 11.5(7)% in energy compared to  $(\pi/2, \pi/2)$ , at odds with spin-wave theory. This is larger than expected from Quantum Monte Carlo simulations and series expansion calculations for the Heisenberg square-lattice antiferromagnet with nearest-neighbor interactions, which predict a zone-boundary dispersion of 8% to 10% [4, 6]. Our observation is opposite to what has been observed in the high-Tc material  $\text{La}_2\text{CuO}_4$  where the energy at  $(\pi, 0)$  is higher than at  $(\pi/2, \pi/2)$  [23]. The latter has been at-

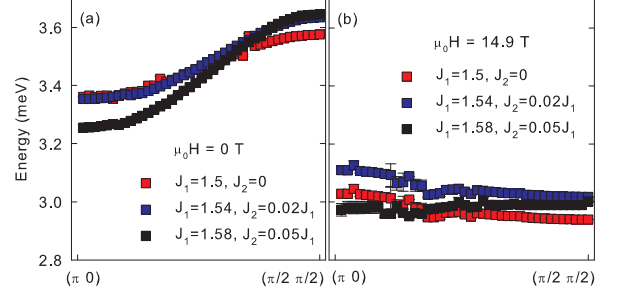


FIG. 2: Series expansion calculations of the zone-boundary dispersion. Theoretical magnon dispersion for different values of the next-nearest neighbor exchange interaction  $J_2$  in zero magnetic field (left panel) and in a  $\mu_0 H = 14.9$  T magnetic field (right panel). The value of the nearest neighbor interaction  $J$  has been normalized to fit the experimental data. The normalization constants are shown in the legend.

tributed to ring-exchanges arising from finite- $U/t$  [24].

We developed series expansion calculations for the  $J_1 - J_2$  model in a magnetic field [25, 26, 27]. Since the magnetic field causes the spins to become non-collinear, this requires the technically difficult multi-block method to be used [27]. Our series expansion calculations for the  $J_1 - J_2$  model [25, 26, 27] show that the addition of  $J_2$  leads to an enhancement of the zone boundary dispersion. Fig. 2 shows the calculated single-magnon energies for different relative strengths  $J_2/J_1$  between nearest to next-nearest neighbor interactions. For  $\text{Cu}(\text{pz})_2(\text{ClO}_4)_2$  we thus attribute the increased zone-boundary dispersion to a small AF next-nearest neighbor interaction of the order of  $J_2 \sim 0.02 - 0.05 J$ .

According to spin wave theory, the energy at  $(\pi/2, \pi/2)$  is equal to  $E_{(\pi/2, \pi/2)} = 2(J_1 - J_2)$  at all fields. Next-nearest neighbor interactions thus lead to a smaller zone-boundary energy, and thus to a smaller effective nearest-neighbor exchange  $J$ . Using  $J = J_1 - J_2$  and  $J = 1.53(8)$  meV determined from susceptibility measurements [20, 22], the field-induced change of  $E_{(\pi/2, \pi/2)}$  is obtained from the field dependence of the renormalization factor  $Z_c = E_{(\pi/2, \pi/2)}/2J$ , yielding  $Z_c = 1.19(2)$  at zero field in excellent agreement the predicted value of  $Z_c = 1.18$  [6].

Fig. 3a shows that the spin excitation at  $(\pi, 0)$  is considerably broader than experimental resolution, and that neutron scattering extends to about  $E = 3.9$  meV. This represents clear experimental evidence of a magnetic continuum at  $(\pi, 0)$  of the square-lattice antiferromagnet that is not expected from spin-wave theory. The continuum is clearly stronger than in copper deuteroformate tetradeuterate (CFDT) with a zone-boundary dispersion of 7% where next-nearest neighbor exchange are absent [9], suggesting that next-nearest neighbor exchange enhances continuum excitations in the 2D  $S=1/2$

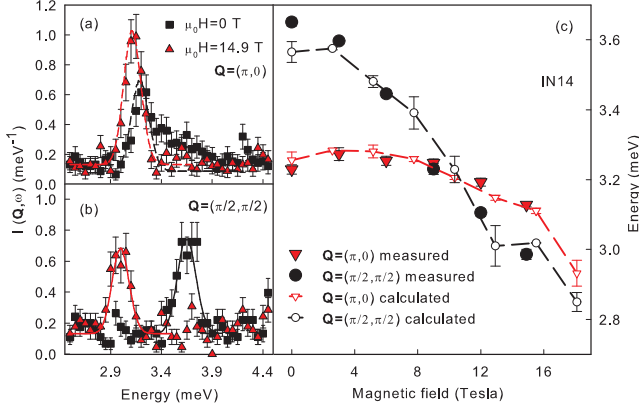


FIG. 3: Field dependence of zone-boundary excitations. Energy scans at  $(\pi, 0)$  and  $(\pi/2, \pi/2)$  are shown in (a) and (b) respectively. The data was measured at  $T = 80$  mK. The black solid line in (b) represents linear spin-wave excitations convoluted with the resolution function. Apart from the continuum region, all the experimentally measured peaks are resolution limited. The field dependent onset of magnetic scattering at  $(\pi, 0)$  and  $(\pi/2, \pi/2)$  as a function of energy is shown in (c) by red triangles and black circles respectively. The dashed red and black lines represent the estimate from the series expansion calculations with  $J_1 = 1.54$  meV and  $J_2 = 0.02J_1$ .

square-lattice antiferromagnet. The extended continuum in  $\text{Cu}(\text{pz})_2(\text{ClO}_4)_2$  is also in contrast to well-defined excitations observed in  $\text{La}_2\text{CuO}_4$  near  $(\pi, 0)$ , suggesting that ring exchange has the opposite effect on the continuum to next-nearest neighbor interactions. Further, Fig. 1 also provides evidence of an energy gap around  $(\pi/2, \pi/2)$  that separates a main mode and a much weaker continuum above 4.2 meV, as predicted by Ho *et al.* [7].

Fig. 3c shows that magnetic fields strongly affect the quantum fluctuations at the zone boundary: The energy of the excitation at  $(\pi/2, \pi/2)$  decreases much faster with field than that at  $(\pi, 0)$ . The zone-boundary dispersion at  $\mu_0 H = 14.9$  T is inverted from that at zero field. Our series expansion calculations show that, with the application of a magnetic field, the inversion of the zone boundary dispersion only occurs for sufficiently small  $J_2/J_1$ . A five percent  $J_2/J_1$  no longer shows the reversal of the dispersion that is seen in experiments. This implies that even a relatively small next-nearest neighbor interactions are effective in enhancing the continuum of excitations, consistent with our estimate that  $J_2/J_1 = 0.02$ . The quantum renormalization factor  $Z_c$  decreases rapidly from  $Z_c = 1.19(2)$  at zero field and approaches  $Z_c = 0.99(2)$  at  $\mu_0 H = 14.9$  T, also consistent with our calculations.

It is known that the wave-vector dependence of the magnetic excitations at the zone boundary is a result of resonating valence bond quantum fluctuations between nearest-neighbor spins that reduce the energy of resonant

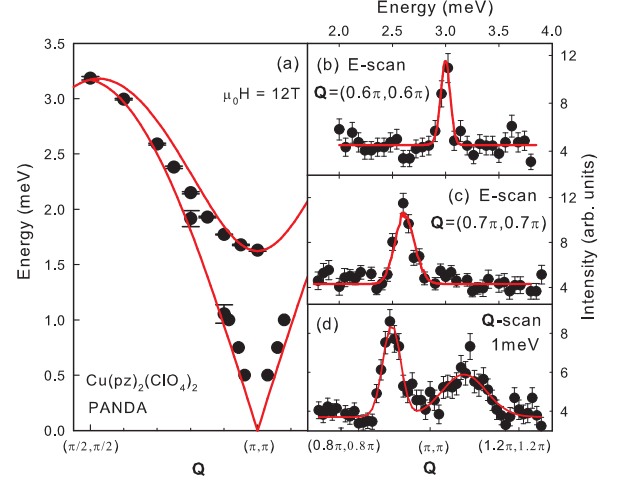


FIG. 4: Spin dispersion for  $H \sim J$ . (a) The spin wave dispersion in  $\text{Cu}(\text{pz})_2(\text{ClO}_4)_2$  measured at  $\mu_0 H = 12$  T and  $T = 80$  mK. The red line represents the spin-wave dispersion with  $J_1 = 1.54$  meV and  $J_2 = 0.02J_1$ . (b,c) Energy scans at  $(0.6\pi, 0.6\pi)$ ,  $(0.7\pi, 0.7\pi)$  provide evidence of a mode with a field-induced gap. (d) Constant-energy scattering at 1 meV energy transfer providing evidence for the Goldstone mode. The solid line in (b)-(d) corresponds to a convolution of a Gaussian with the resolution function, demonstrating that the excitations are resolution limited.

excitations near  $(\pi, 0)$  below what is expected from renormalized spin-wave theory [6, 9]. The field-induced reversal of the zone-boundary dispersion reveals that magnetic fields of the order of  $H \sim J$  strongly couple to these local quantum fluctuations. This dispersion, that is not expected from spin-wave theory, demonstrates the presence of local quantum fluctuations in the 2D  $S=1/2$  square-lattice antiferromagnet even for fields of the order of  $H \sim J$ . The quantum origin of the dispersion reversal is also confirmed by our series expansion calculations. The observed dispersion suggests that the energy of the resonance at  $(\pi, 0)$  is raised by 4.5(7)% above that of renormalized spin-wave theory, providing direct evidence of field-tuned resonating valence bond fluctuations.

The excitation spectrum at  $\mu_0 H = 12$  T features two well defined magnetic modes of excitations (Fig. 4). The spectrum consists of a Goldstone mode, that indicates unbroken rotational spin symmetry in the plane perpendicular to the magnetic field, and a gapped mode. The field dependence of the mass of gapped mode at the AF zone center, shown in Fig. 5, is linear, which is consistent with the theoretical arguments discussed in [28]. However the finite gap at zero field, obtained by the linear fit to the experimental data, implies the existence of a small anisotropy in the system and requires additional investigations. We also analyzed the spectral weight of the gapped excitation at  $(\pi, \pi)$ . Our calculations completely describe the observed field dependence of the peak inten-

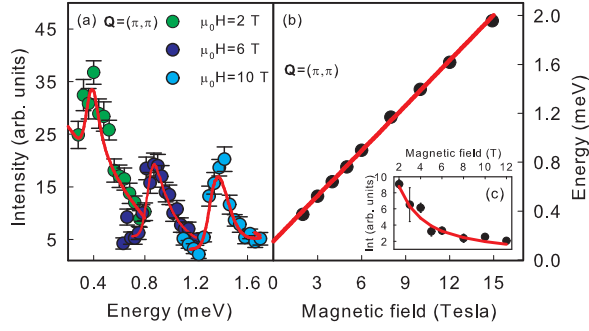


FIG. 5: Field dependence of the zone-center excitation. Energy scans performed at  $(\pi, \pi)$  at  $\mu_0 H = 2$  T,  $\mu_0 H = 6$  T,  $\mu_0 H = 10$  T (a) and the gap energy at the AF point plotted as the function of field (b). The data was measured at  $T = 80$  mK. The solid lines in (a) are the fits of a Gaussian function convoluted with the resolution function. The filled circles in (b) represent the experimental data. The solid line in (b) is the linear fit of the gap energy. Black circles in inset (c) show the measured intensities as function of magnetic field and the curve is the scattering intensity calculated using linear spin-wave theory.

sities of the gapped mode at the AF zone center (Fig. 5c).

Fig. 4 shows the observed dispersion from  $(\pi, \pi)$  to  $(\pi/2, \pi/2)$  compared to linear spin-wave theory. The linear spin-wave theory calculations in a magnetic field was performed for the following Hamiltonian:

$$\mathcal{H} = J_1 \sum_{\langle i, j \rangle} \mathbf{S}_i \cdot \mathbf{S}_j + J_2 \sum_{\langle i, k \rangle} \mathbf{S}_i \cdot \mathbf{S}_k - \mu_0 H \sum_i \mathbf{S}_i^a, \quad (1)$$

where  $\langle i, j \rangle$  represents nearest neighbor pairs of spins,  $\langle i, k \rangle$  next nearest neighbor pairs and  $\mathbf{S}^a$  is a spin component perpendicular to the  $bc$  plane. The renormalized spin wave theory with  $J_{\text{eff}} = 1.54(1)\text{meV}$  and  $Z_c = 1.03(1)$  for  $\mu_0 H = 12$  T describes qualitatively the observed dispersion, as shown in Fig. 4(a). However, for wave-vectors near  $(3\pi/4, 3\pi/4)$ , spin-wave theory clearly predicts a larger spin-wave energy than experimentally observed. This difference may reflect the importance of magnon-magnon interactions [14, 15]. Possibly, better agreement could be obtained by including higher-order terms in the spin-wave calculation.

In summary, our study shows that the zone-boundary dispersion and the zone-boundary continuum of the 2D  $S=1/2$  square-lattice antiferromagnet are enhanced by next-nearest neighbor interactions, while the spin-wave energies merely experience a small renormalization. Magnetic fields of the order of  $H \sim J$  lead to a qualitative change of the quantum fluctuations that suppress the continuum of excitations and renormalize the spin-wave velocity, but without suppressing the zone-boundary dispersion that arises from non-trivial quantum fluctuations. In fact, in contrast to spin-wave theory, we find

that the zone-boundary dispersion is inverted compared to zero field, providing direct evidence of a field-induced change of resonating valence bond fluctuations.

We thank Dirk Eitzdorf and Harald Schneider for technical assistance at PANDA spectrometer at FRM2 and the technical services of ILL involved during the experiment at IN14. This work was supported by the Swiss NSF (Contract No. PP002-102831).

After submission of our manuscript, we became aware of A. Lüscher and A. Laeuchli [29] who also find theoretically that the zone boundary dispersion inverts as a function of field.

- 
- [1] L. D. Faddeev, L. A. Takhtajan, Phys. Lett. **85** 375 (1981).
  - [2] F. D. M. Haldane, Phys. Rev. Lett. **50**, 1153 (1983).
  - [3] A. W. Sandvik, Phys. Rev. B **56**, 11678 (1997).
  - [4] W. Zheng, J. Oitmaa, C. J. Hamer, Phys. Rev. B **71**, 184440 (2005).
  - [5] R. R. P. Singh, M. P. Gelfand, Phys. Rev. B **52**, R15695 (1995).
  - [6] A. W. Sandvik, R. R. P. Singh, Phys. Rev. Lett. **86**, 528 (2001).
  - [7] C. M. Ho *et al.* Phys. Rev. Lett. **86**, 1626 (2001).
  - [8] N. B. Christensen *et al.* J. Mag. Magn. Mater. **272**, 896 (2004).
  - [9] N. B. Christensen *et al.* Proc. Natl. Acad. Sci. U.S.A. **104** 15264 (2007).
  - [10] H. M. Rønnow *et al.* Phys. Rev. Lett. **87**, 037202 (2001).
  - [11] Y. J. Kim *et al.* Phys. Rev. B **64** 024435 (2001).
  - [12] M. D. Lumsden *et al.* Phys. Rev. B **74** 214424 (2006).
  - [13] P. Chandra, B. Doucot, Phys. Rev. B **38**, 9335 (1988).
  - [14] M. E. Zhitomirsky, T. Nikuni, Phys. Rev. B **57**, 5013 (1998).
  - [15] M. E. Zhitomirsky, A. L. Chernyshev, Phys. Rev. Lett. **82**, 4536 (1999).
  - [16] O. F. Syljuåsen, Phys. Rev. B **78**, 180413 (2008).
  - [17] B. Schmidt, P. Thalmeier, N. Shannon Phys. Rev. B **76** 125113 (2007).
  - [18] P. Thalmeier, M. E. Zhitomirsky, B. Schmidt, N. Shannon, **77** 104441 (2008).
  - [19] N. Read, S. Sachdev, Phys. Rev. Lett. **66**, 1773 (1991).
  - [20] F. M. Woodward *et al.* Inorg. Chem. **46**, 4256 (2007).
  - [21] M. M. Turnbull *et al.* Mol. Cryst. Liq. Cryst. Sci. Technol. Sect. A **334**, 957 (1999).
  - [22] T. Lancaster *et al.* Phys. Rev. B **75**, 094421 (2007).
  - [23] R. Coldea *et al.* Phys. Rev. Lett. **86**, 5377 (2001).
  - [24] W. Zheng *et al.* Phys. Rev. B **72**, 033107 (2005).
  - [25] M. P. Gelfand, R. R. P. Singh, Adv. Phys. **49**, 93(2000).
  - [26] J. Oitmaa, C. Hamer, W. Zheng, *Series Expansion Methods for strongly interacting lattice models* (Cambridge University Press, 2006).
  - [27] W. Zheng *et al.* Phys. Rev. B **63**, 144410 (2001).
  - [28] D.I. Golosov and A.V. Chubukov, Sov. Phys. Solid State **30**, 893 (1988).
  - [29] A. Lüscher and A. Laeuchli, arXiv:0812.3420